Intelligent fault diagnosis and protection in DG-connected systems using resistive superconducting fault current limiter and ANN-based detection

Lekshmi R. Chandran[1], Ilango Karuppasamy[2], Manjula G. Nair[1]
[1]Department of Electrical and Electronics Engineering, Amrita Vishwa Vidyapeetham, Amritapuri, India
[2]Department of Electrical and Electronics Engineering, Amrita School of Engineering, Amrita Vishwa Vidyapeetham, Coimbatore, India

Article Info

Article history:

Received Jun 16, 2025
Revised May 12, 2026
Accepted Jun 9, 2026

Keywords:

Artificial neural network
Distributed generation
Fault diagnosis
Superconducting fault current limiter
Symmetrical components

ABSTRACT

Ensuring reliable fault diagnosis and rapid recovery in distributed generator (DG)-connected distribution systems is critical, as the integration of DG sources significantly elevates fault current levels. This study proposes an integrated approach that combines a resistive superconducting fault current limiter (RSFCL) with an artificial neural network (ANN)-based intelligent fault diagnosis framework. The objective is to limit excessive fault currents while improving detection accuracy under varying network configurations. The RSFCL is strategically placed by analyzing fault current magnitude, voltage quality, and resistance value to achieve effective current limitation without compromising system stability. Meanwhile, the ANN employs symmetrical components of current and voltage as diagnostic features. To enhance robustness, correlated variables are identified and eliminated during feature selection, strengthening the model’s fault discrimination capability. Simulation results demonstrate that the optimal RSFCL placement reduces fault current contribution ratios by up to 82.16% under symmetrical fault conditions. The ANN-based fault detection model achieves a validation accuracy of 99.7%, outperforming conventional threshold-based methods by minimizing nuisance tripping and improving circuit breaker coordination. Overall, the combined RSFCL–ANN framework provides an effective and intelligent solution for fault diagnosis and protection in DG-integrated power systems.

Corresponding Author:

Lekshmi R. Chandran
Department of Electrical and Electronics Engineering, Amrita Vishwa Vidyapeetham
Amritapuri Campus Amritapuri, Clappana P. O., Kollam – 690525, Kerala, India
Email: lekshmichandran@am.amrita.edu

1. INTRODUCTION

The integration of distributed generations (DG) into distribution systems has become necessary due to the rising power demand, power loss in long transmission lines, and the emergence of decentralized power generation. The distribution system is connected to DG units, such as photovoltaic (PV) systems, wind turbines, and energy storage, using a variety of devices, such as circuit breakers, solid-state breakers, or power electronics interfaces. Although DG increases system reliability, it can also increase short-circuit current and harmonic pollution, especially when linked to power electronic interfaces. These interfaces also make it easier for false feeder trips, loss of relay coordination, overvoltage, and unwanted islanding to occur [1]-[3]. Monitoring and protection issues arise with the integration of distributed generations (DG) into the electrical distribution system. The use of current limiting fuses, circuit breakers made to handle extremely high fault currents, feeder splitting, high impedance transformers, raising generation voltage, air core reactors, and series reactors are just a few of the techniques used to ensure safe operation in power systems. Passive fault current limitation methods introduce impedance in normal and fault conditions and can create power quality issues and stability issues. Whereas active techniques establish a small impedance during normal operating conditions and a high impedance under faulty conditions [3]-[5].

Fault current limiters (FCLs) as low impedance elements in normal operation and provide high impedance during faults to limit high fault currents to an acceptable level. The generalized FCL operation during normal and fault conditions is shown in Figure 1 [6]. FCL installation reduces stress on safety equipment by reducing short-circuit current and improving voltage quality in the system. FCLs are classified as superconducting fault current limiters (SFCLs) and non-superconducting FCLs based on their material. Fault current limiters such as pyrotechnic fault current limiters (Is-limiters), superconducting FCL- magnetic, transformer, resistive, flux lock type, solid-state FCL, fault current limiting reactor (FCLR), electromagnetic FCL, hybrid FCL are reported in various research works [7]-[15]. SFCL can be effectively used for fault current limitation without any degradation in high voltage AC grid, DC grid, and interconnected hybrid grid [16]-[18]. According to studies, SFCL may reduce both transient and sustained fault currents in an interconnected system and has a fast response time. Studies show that by choosing circuit breakers with lower current capacities and coordinating their use, SFCL also enhances the system [19]-[21]. Superconductor nonlinearity and power handling capacity are used for FCL. Superconductors' nonlinear response to fluctuations in current, temperature, and magnetic field determines the fault currents limiting [20]-[24]. As any of these parameter's change, the superconductor switches from its usual operating regime to a superconducting one. Liquid nitrogen is often used as a coolant for HTS SFCL. Some of the extensively used HTS superconducting material combinations used in industrial applications are Bismut-Strontium-Calcium-Copper-Oxide (compound of Bi-2212/Bi-2223) and Yittrium-Barium-Copper-Oxide (YBCO) [23]-[25]. Fault current limiters (FCLs) are still being developed and researched at various levels using cutting-edge technologies, including solid-state and superconducting materials. Fault current limiters (FCLs) are still being developed and researched at various levels using cutting-edge technologies, including solid-state and superconducting materials. Due to their simple design and rapid reduction of fault currents, resistive superconducting fault current limiters (RSFCLs) stand out among them. RSFCLs are a desirable option for use in the current investigation due to these qualities.

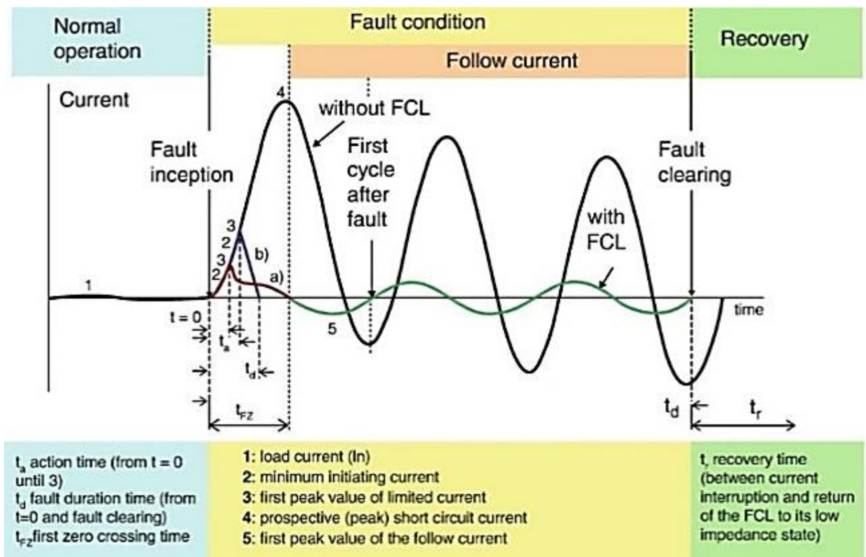

Figure 1. Current interruption characteristics of FCL in general [6]

Protection enhancement is not limited to a reduction in fault current level. An intelligent monitoring and diagnosis system to distinguish the system's normal operation and abnormal operation in a changing environment is also very crucial. Machine learning and AI-based algorithms are becoming popular due to their adaptiveness and implementation efficiency for fault detection and diagnosis. MLP, deep neural networks, KNN, decision tree models, with specific features are used as AI models for different fault classification applications [26]-[30]. ANN-based fault diagnosis systems are used in this work since they can be trained with changing network parameters with less complexity.

The proposed system is structured into two distinct phases, each making significant contributions to the overall research endeavor: i) Firstly, the work focuses on the study of bus voltage and current by placing the resistive superconducting fault current limiter (RSFCL) in different locations within the distribution system. This placement is determined by considering three critical factors: the magnitude of fault current, voltage quality, and resistance value. By assessing the effectiveness of the RSFCL in limiting fault currents and enhancing voltage quality, the study establishes a comprehensive framework for its application in DG-assisted radial distribution systems. ii) Secondly, the research employs an artificial neural network (ANN) based fault diagnosis technique, utilizing the symmetrical components of current and voltage as key electrical signature features. This innovative approach enables accurate detection and identification of faults within the system. By leveraging the inherent characteristics of symmetrical components, the ANN-based fault diagnosis scheme offers a robust solution for fault detection, contributing to the overall reliability and efficiency of the proposed system. The ANN reduces the nuisance trips of the circuit breaker by providing an additional layer of fault detection beyond the preset thresholds.

Together, these contributions enhance the fault management capabilities of DG-assisted radial distribution systems, paving the way for improved system performance. The rest of this work is organized as follows. Section 2 gives the operation, related work, and analysis of RSFCL in the test system. Section 3 defines the ANN architecture, related works, and proposed fault diagnosis model. Section 4 defines the integrated system approach. The conclusion is presented in section 5.

2. RESISTIVE SUPERCONDUCTING FAULT CURRENT LIMITER IN DISTRIBUTION SYSTEM

A resistive superconducting fault current limiter (RSFCL), as shown in Figure 2, with modelling as in (1), is used in this work due to the simplicity of modeling and fast response. The resistive superconducting fault current limiter consists of a superconducting element (HTS) housed in a vacuum-insulated container filled with coolant. It is connected in series with the power distribution network. During normal operation, the RSFCL has a small resistance (R_{FCL}) and dissipates low energy. However, when a fault occurs, the current (I_{FCL}) exceeds the critical current value, causing RFCL to increase exponentially. This leads to the heating of the superconductor above its critical temperature (T_c), causing a transition from its superconducting state to a highly resistive state. As a result, the RSFCL effectively reduces the fault current by exploiting the phenomenon known as "quench of superconductors". Once the fault current decreases, the superconducting material is cooled using cryogenics, allowing R_{FCL} to return to its superconducting state. The parallel resistance (R_{sh}) helps distribute heat during the quench, regulates the current limitation, and prevents over-voltage due to the fast current limitations [25], [31]-[38]. RSFCL is modeled as a nonlinear resistance depending on time as in (1) [25], [35], [36].

$$R_{FCL}(t) = \begin{cases} 0 & t < t_{a0} \\ R_{FCL}\left[1 - \exp^{\left(-\frac{t-tao}{\tau}\right)}\right]^{1/2} & t_{a0} \le t < t_{a1} \\ a_1(t - t_{a1}) + b_1 & t_{a1} \le t < t_{a2} \\ a_2(t - t_{a2}) + b_2 & t_{a2} \le t \end{cases} \quad (1)$$

Where R_{FCL} is the nominal state resistance of RSFCL, τ is the time constant, t_{a0} is the quench-starting time, t_{a1} is the first-stage recovery-starting time, t_{a2} is the secondary-stage recovery-starting time, and t completed recovery time. a_1, a_2, b_1, and b_2 are expressed as the model coefficients.

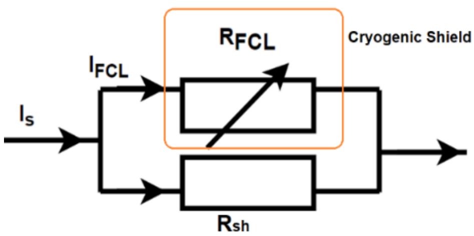

Figure 2. Superconducting resistive fault current limiter

The effectiveness of resistive superconducting fault current limiters to improve the voltage quality issues like voltage sag and voltage swell is studied in [32]. RSFCL made with YBCO shows better transient stability performance in a multi-machine power system than I-SFCL in a comparative study with YBCO and Bi2212 [24], [25]. The comparative analysis of different location placements of RSFCL and ISFCL for transient stability improvement shows that the system behaves better when RSFCL is better than ISFCL, irrespective of its location [39]. Whereas according to a study in [33], the optimal sizing and allocation had a considerable effect on better performance to the security of the network. The best practices of FCL implementation in the UK and the USA reported their effectiveness in system resilience and protection improvement [40]-[43].

Fault current reduction capability, voltage quality improvement, and minimal superconducting fault current resistance factors are considered for the placement of RSFCL in the given system in this work. The resistance value of RFSCL is considered since the cost of installation is highly dependent on the resistance value. The higher the resistance value higher the installation cost.

The test system to study the effectiveness of RFSCL in a DG-connected distribution system is shown in Figure 3 with parameters as shown in Table 1. DG's mentioned in this study can be a representation of solar/wind/any local generation. Table 2 shows the symmetrical and unsymmetrical fault currents observed near the 11 kV/415 V distribution transformer before and after the installation of DG at the P3 location of the system. It is observed that the installation of DG causes the fault current to increase abnormally. The distribution system is then analyzed for fault current limiting ability, grid voltage quality, and minimum value of RSFCL at different allocations of RSFCL with positions P1, P2, P3, P1-P2, and P1-P3.

The performance analysis of the system is studied using parameters current reduction ratio and voltage sag Percentage for symmetrical faults at F1 and F2 using (2) and (3).

$$\text{Current Reduction Ratio (CRR)} = \frac{I_{sfault} - I_{sfcl}}{I_{sfault}} \tag{2}$$

$$\text{Voltage Sag Percentage(VSP)} = \left(\frac{V_{nom} - V_{sfault}}{V_{nom}}\right) x100 \tag{3}$$

Where I_{sfault} is rms value of fault current without RSFCL, I_{sfcl} rms value of fault current with RSFCL, V_{sfault} is rms line voltage of system during fault, V_{nom} is nominal rms system voltage.

Table 1. Test system parameters

Parameters	Value
Distribution system voltage (line to line, RMS)	11 kV
Nominal system frequency	50 Hz
Source X/R ratio	7
Transformer 1	100 MVA, 33 kV/11 kV
Transformer 2	250 KVA, 11 kV/415 V
Distribution generator	50 kW-5 kVAR
Net domestic and commercial loads	60 kW, 10 kVAR
Net industrial loads	45 kW, 2 kVAR

Table 2. Peak RMS of fault current of the test system with and without DG

Fault position	F1				F2			
Fault type	Without DG		With DG		Without DG		With DG	
	I_{max} (A)	I_{min} (A)	I_{max} (A)	I_{min} (A)	I_{max} (A)	I_{min} (A)	I_{max} (A)	I_{min} (A)
Symmetrical fault (ABCG)	4220	3560	4550	4125	4400	3500	4560	4100
Asymmetrical fault (AG)	2654	1550	3100	2079	2600	1440	2995	2025

Table 3 (see Appendix) shows the performance analysis of the system for symmetrical faults F1 and F2 with RFSCL placed at different positions. The various observations for each RFSCL position based on the provided symmetrical fault F1 and F2 scenarios are as follows:

i) P1 position: The P1 position demonstrates a strong ability to reduce fault currents, with the current reduction ratio (CRR) reaching 67.93% at a resistance of 40 Ω for both F1 and F2 scenarios. It also maintains voltage quality well, evidenced by a low voltage sag percentage (VSP) of 2.64% at the same resistance level. This indicates that P1 is effective in both current limitation and voltage stabilization.

ii) P2 position: The P2 position has no impact on fault current reduction in the F1 scenario, but it shows a marked improvement in the F2 scenario as resistance increases. Specifically, at 40 Ω, it achieves a CRR of 87.26% and a VSP of 1.73% for F2, showcasing its potential for significant current limitation and voltage quality maintenance under certain fault conditions. However, the performance is highly dependent on the fault type, which may limit its broader applicability.

iii) P3 position: The P3 position is less effective compared to P1, with CRR values considerably lower and VSP figures that remain relatively high across all resistance values for both fault scenarios. At 40 Ω, the CRR is around 12% for both F1 and F2, and the VSP is 99.18%, indicating that P3 is not as capable in managing fault currents or maintaining voltage quality as the other positions.

iv) P1-P2 position: Combining P1 and P2 positions offers a balanced solution. At a resistance of 40 Ω, the combined P1-P2 position delivers a high CRR of around 67% for F1 and 89% for F2, along with a low VSP of 2.64% for both faults. This combination emerges as a strong contender for RFSCL placement, achieving significant current reduction and good voltage stabilization.

v) P2-P3 position: P2-P3, while offering improvements in fault current reduction in the F2 scenario, does not provide as compelling results in the F1 scenario, with no impact on fault current reduction observed. The effectiveness of this position combination is more pronounced in the F2 scenario, where at 20 Ω, a CRR of over 75% is achieved, although this is less than what is seen in the P1-P2 combination.

vi) P1-P3 position: This position provides a notable CRR for both F1 and F2 at moderate resistance values, maintaining good voltage quality at higher resistance levels. This suggests that the P1-P3 combination could be considered for RFSCL placement, especially at a resistance level of around 40 Ω, which balances performance with cost considerations.

vii) P1-P2-P3 position: While the P1-P2-P3 position demonstrates high CRR values at higher resistances, it may not be as cost-effective due to the implications of installing RFSCLs across multiple locations. The performance at higher resistances is optimal, but for cost-effectiveness, the recommendation is to consider other position combinations.

viii) A tradeoff is considered for the proper placement of accounting fault current limiting ability, grid voltage quality, and minimum value of RSFCL. Thus, position P1-P2 with a maximum resistance of 20 Ω is selected based on this tradeoff. At 20 Ω resistance, P1-P2 shows a CRR of 57.79% for symmetrical fault F1 and 82.16% for symmetrical fault F2. This indicates a high efficacy in limiting the fault current for both types of faults.

A reduction of over 50% in fault current is significant and implies that the protective equipment and the rest of the system are subjected to much lower stress during fault conditions. The VSP at 20 Ω for P1-P2 is 8.09% for F1 and -3.27% for F2. A VSP of 8.09% suggests that the voltage sag is within acceptable limits, maintaining grid stability close to the nominal voltage during a fault. The VSP goes slightly negative (-1.91%), which might imply a slight overvoltage condition, but still suggests good voltage control during faults. Lower resistance values usually translate into lower material costs and potentially reduced cooling requirements, thus resulting in overall savings in the implementation and operational phases. The fault current reduction and voltage quality improvement are observed in all fault cases. The voltage quality of the system can further be improved using power compensators.

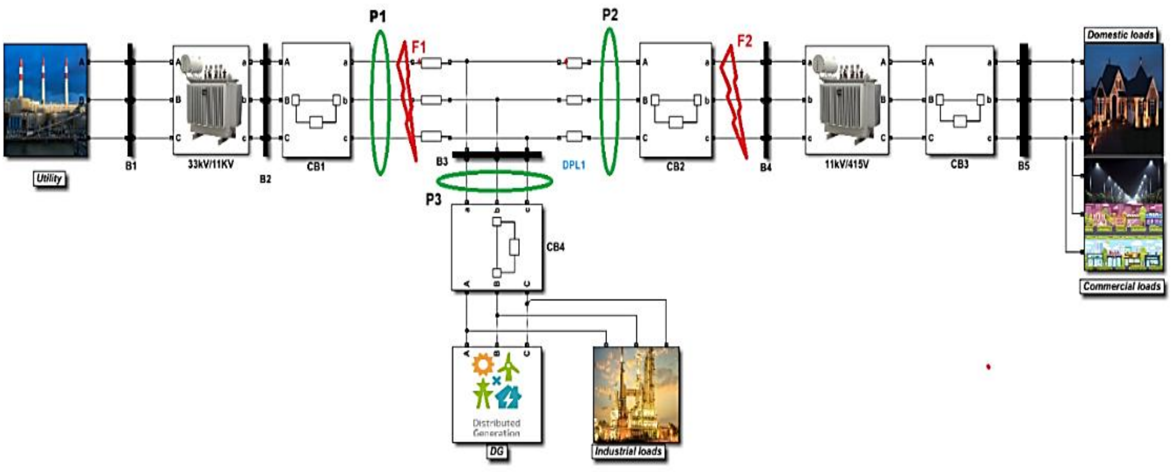

Figure 3. Test system of the DG-connected distribution system

3. PROPOSED FAULT DIAGNOSIS METHODOLOGY: INTELLIGENT FAULT DIAGNOSIS USING ARTIFICIAL NEURAL NETWORK

Intelligent systems are more widely used nowadays since they can operate autonomously, with higher levels of accuracy and reliability. An artificial neural network (ANN) aided intelligent fault diagnosis is also modeled in this study, along with the protection enhancement of the system using RFSCL. Unsymmetrical fault analysis without considering symmetrical faults using ANN is mentioned in the work [44]. Transmission line fault detection and location identification with RMS values of current and voltage as feature variables is mentioned in the work [45]. ANN and wavelet-based fault identification and localization are analyzed in the work [46]. Ant colony optimization-based wavelet transform and ANN to detect faults in HVDC transmission lines is mentioned in the work [47]. High impedance fault detection using discrete wavelet and decision tree, fault detection and location prediction using space vector machine (SVM) and Gaussian regression, adaptive fuzzy-based relay protection, and several machine learning algorithms are also mentioned in various works [48]-[50]. ANN-based fault identification uses RMS values or wavelet coefficients, or their static or dynamic feature derivatives, as the features for training. Wavelet-based fault classification using SVM [51] and ANN [52] for transmission lines has been studied. The study in [53] analyzes fault detection and classification in compensated transmission lines using instantaneous voltage and current signals. PCA-based feature extraction reduces dimensionality, capturing key time-frequency features.

Machine learning classifiers (KNN, MNN, QSVM) are compared, with QSVM achieving 99.3% accuracy. The various features used for training in studies [44]-[53] are mainly instantaneous values, RMS values, and wavelet coefficients, or their statistical derivatives of either voltage or current or both. The electrical signature features identified for the current work are the symmetrical components of voltage and current. Assuming S_A, S_B, and S_C are the phase voltages (or currents) of an unbalanced three-phase system, the transformation to symmetrical components can be represented by (4).

$$\begin{bmatrix} S_1 \\ S_2 \\ S_0 \end{bmatrix} = \frac{1}{3}\begin{bmatrix} 1 & a^2 & a \\ 1 & a & a^2 \\ 1 & 1 & 1 \end{bmatrix}\begin{bmatrix} S_A \\ S_B \\ S_C \end{bmatrix} \tag{4}$$

S_1, S_2, S_0 represent the positive, negative, and zero sequence components, respectively, and a is the complex operator defined as $a = \cos(120°) + j\sin(120°)$.

The collective information about these feature variables communicated to the utility center helps in identifying the type and zone/location of the fault. This concept of intelligent fault diagnosis by utility centers using symmetrical components of voltage and current is the focus of this research work.

The methodology for developing and implementing the intelligent fault detector using ANN is illustrated in Figure 4. It consists of the following steps:

- Step 1: Data collection: Three-phase instantaneous voltage and current data at bus 2 and bus 4 of the test system (as in Figure 3) are collected for normal and various fault conditions. The fault conditions are created by varying fault resistance, load, and DG levels at different fault locations.
- Step 2: Feature extraction: Symmetrical components of voltage and current at bus 2 and bus 4 for faults at F1 and F2, both in the presence and absence of DG and RSFCL, are analyzed and extracted. This process involves analyzing the data during fault and pre-fault conditions. A dataset of 2500 samples per label is collected as input features for training the ANN model.
- Step 3: Normalization and transformation: The input features are normalized and transformed to a range of -1 to +1. This normalization process helps improve the performance of the neural networks.
- Step 4: Fault labeling: Different fault conditions, such as symmetrical faults, unsymmetrical faults, and no faults at bus 2 (Zone 1) and bus 4 (Zone 4), are labeled as F1 to F23. One-hot encoding is used to represent the fault labels/targets in this study.
- Step 5: ANN training: The ANN model is trained by tuning the model parameters and hyperparameters until the desired network setting parameters are achieved. The neural network's weights and biases are adjusted during this process to minimize the error between predicted and actual fault labels. 70% of the data is used for training and 30% for testing.
- Step 6: Test and performance analysis: The trained ANN model is tested using unseen data to evaluate its performance. Performance metrics such as precision, recall, and F1-score are calculated to assess the effectiveness of the model in detecting and classifying faults.
- Step 7: Selection and deployment: Based on the performance analysis, the best-performing ANN model is selected and deployed for real-world fault detection in DG-connected distribution systems.

Multi-collinearity effect of feature variables is analyzed using bivariate correlation. Highly dependent feature variables have high correlation values. In such cases, one of the variables can be eliminated. Figure 5 shows the correlation graph and pair plot of all 12 feature variables. The variables (12 n, v2n) are highly correlated with a correlation of 0.81. Hence, v2n is dropped from further training of the system. A dense neural network is used for modeling in this work [47], [54].

The general structure of the dense artificial neural network (ANN) model can be represented as follows. Input vector with number of feature inputs I, is $x \epsilon R^I$. For the l^{th} hidden layer with N_l number of neurons, the output is calculated using the formula as in (5).

$$h^{(l)} = f^{(l)}\left(W^{(l)T}h^{(l-1)} + b^{(l)}\right)\ (where\ h^{(0)} = x) \tag{5}$$

Where the hidden layer weight matrix is $W^{(l)} \epsilon\ R^{N_{t-1}\ X\ N_l}\ (where\ N_0 = I)$ and bias matrix is $b^{(l)} \in R^{N_l}$.

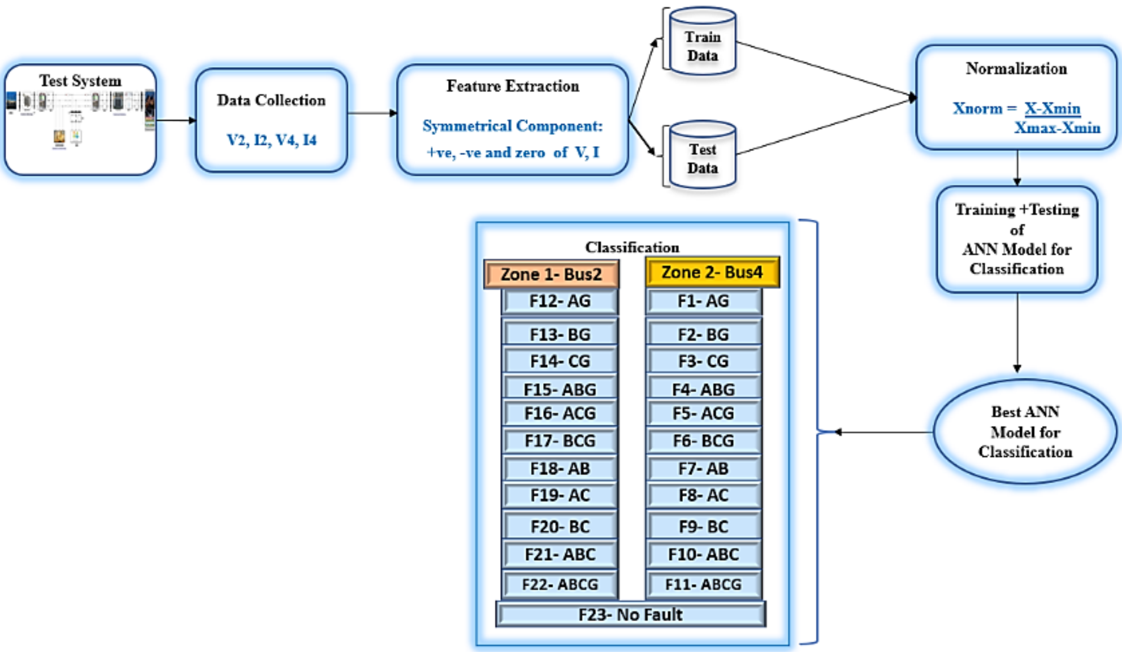

Figure 4. ANN-based fault diagnosis system

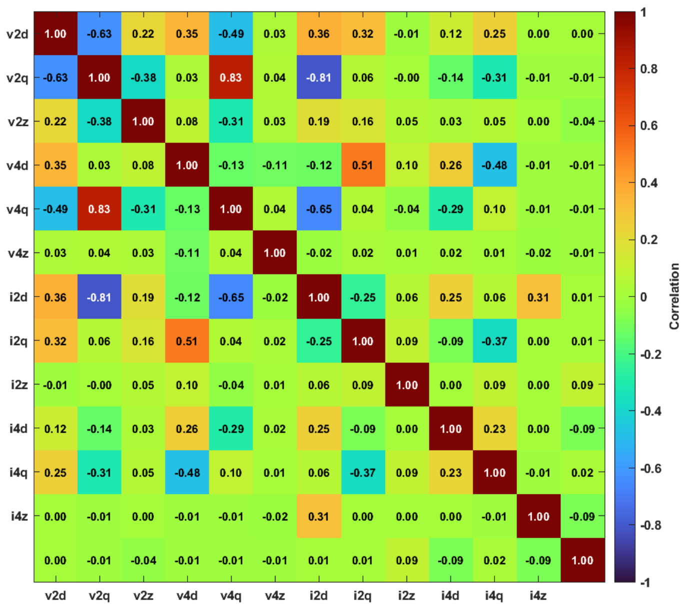

Figure 5. Correlation graph of feature variables

The output vector y in the output layer is calculated using the formula as in (6).

$$y = f^{(o)}\left(W^{(o)T} h^{(L)} + b^{(o)}\right) \tag{6}$$

Where the output weight matrix is $W^{(o)} \epsilon\ R^{N_L\ X\ o}$ and the bias matrix is $b^{(o)} \in R^o$, L is the number of hidden layers and o is the number of output classes. The rectified linear unit (ReLU) activation function, represented as $f^{(l)}$ used in hidden layers is defined as in (7). The SoftMax activation function in the output layer transforms the output into a probability distribution over the 23 output classes.

$$f(z)^{(l)} = \max(0, z) \tag{7}$$

4. RESULTS AND ANALYSIS

The test system with RFSCL placed at the position P1-P2 in a DG-connected distribution system, as shown in Figure 3, with parameters as shown in Table 1, is analyzed for various fault classifications using different ANN models. The size of the input layer of the ANN depends on the input features, and the output layer depends on the target. A dropout of 0.2 is used for regularization. The training of the ANN involves adjusting the weights and biases to minimize the cross-entropy loss function. ANN models used for training the model are shown in Table 4. Model 6 shows 99.7% accuracy. Model 6 is selected for deployment based on the accuracy.

Performance metrics used for evaluation of ANN, such as precision, recall, and F1-Score, are calculated as in (8)-(10).

$$\text{Precision} = \frac{\text{PT}}{\text{PT+PF}} \tag{8}$$

$$\text{Recall} = \frac{\text{PT}}{\text{PT+NF}} \tag{9}$$

$$\text{F1} - \text{Score} = \frac{2*\text{PT}}{2*\text{PT+PF+NF}} \tag{10}$$

Where PT is true positive, PF is false positive, and NF is false negative.

Figure 6 shows the performance metrics of a classification model for different types of faults (F1 to F23), using three key evaluation criteria: precision, recall, and the F1 score using model 6. The majority of the fault types (F2 to F9, F12 to F20, and F23) have perfect scores (1.00) in precision, recall, and F1 score. Fault types F1, F10, F11, F21, and F22 show slightly lower scores in one or more metrics, but these scores are still very high (all above 0.93). The F1 score, which is the harmonic mean of precision and recall, is very high for all fault types, with the lowest being 0.96. This indicates a well-balanced model that is effective in both identifying the correct fault types (precision) and covering all actual instances of each fault type (recall). ANN model 6 demonstrates exceptional effectiveness in fault diagnosis with a training accuracy of 98.6% and validation accuracy of 99.7%. The ability to accurately classify a wide variety of fault types is indicative of a robust and reliable diagnostic tool. Previous studies have reported high classification accuracy using ANN models, including 100% accuracy with instantaneous voltage and current as features [55], and a mean squared error (MSE) of 0.011189 when using RMS values of current and voltage [45]. The present work introduces a novel selection of feature variables (symmetrical components of voltage and currents), explicitly addresses multicollinearity, and reduces feature redundancy. Furthermore, it expands the scope by incorporating a greater number of fault classes (12 classes per zone), achieving improved accuracy.

Table 1. Comparison of dense ANN models

Parameter	Model 1	Model 2	Model 3	Model 4	Model 5	Model 6
No of feature inputs	11	11	11	11	11	11
No of hidden layers -2	2	2	2	2	2	2
No of neurons in dense hidden layer-1	10	12	10	12	24	48
No of neurons in dense hidden layer-2	10	12	20	24	48	48
Activation function in hidden layer	Relu	Relu	Relu	Relu	Relu	Relu
Activation function in output layer	Softmax	Softmax	Softmax	Softmax	Softmax	Softmax
No of outputs	23	23	23	23	23	23
Learning rate	0.01	0.01	0.01	0.01	0.01	0.01
Optimizer	Adam	Adam	Adam	Adam	Adam	Adam
Drop out	0.2	0.2	0.2	0.2	0.2	0.2
Epochs	50	50	50	50	50	50
Training accuracy (%)	68	76	83.7	87	97.7	98.6
Validation accuracy (%)	78	84	90	82	99	99.7

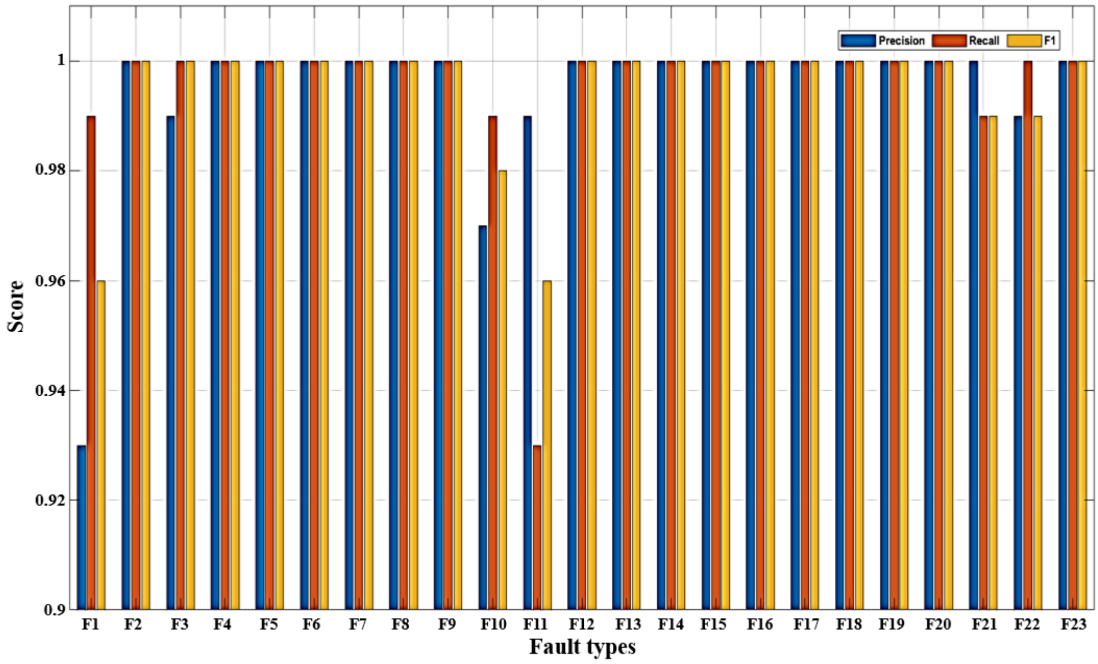

Figure 6. Performance metric of model 6

In this study, RSFCL is placed in the system considering fault reduction capability, grid voltage quality, and reduced resistance to limit the fault currents. The sensitivity and nuisance tripping of the circuit breaker in a DG-connected system are normally addressed using adaptive and non-adaptive protection coordination methods [56], [57]. Fault current limiters (FCL) can be placed to reduce the extra fault current contributed by the DG and maintain the preset relay setting. Adaptive protection schemes without FCL [58], [59] or with FCL [60]-[63] can be used to improve the sensitivity. This study also introduces a non-adaptive protection approach to reduce the nuisance tripping of circuit breakers (CBs) by integrating an Artificial Neural Network-based classifier decision along with the conventional relay logic for circuit breakers. Figure 7 shows the integrated system concept to reduce the nuisance tripping of the circuit breaker. When a fault is confirmed, the ANN signals the nearest CB to isolate the fault. This response is carefully coordinated with other CBs along the line, maintaining a coordination time interval (CTI) of 0.3 seconds to ensure that the nearest breaker to the fault trips first, localizing the fault and minimizing its impact on the network. The decision to trip a CB is based on the ANN's confirmation, enhancing the decision's accuracy beyond traditional detection methods, which rely solely on predefined settings. The time dial (TD) and plug setting (PS) of each relay for circuit breakers using the standard inverse curve and CT ratio of 200/5 A for systems with and without RSFCL are shown in Table 5 for a CTI of 0.3 s.

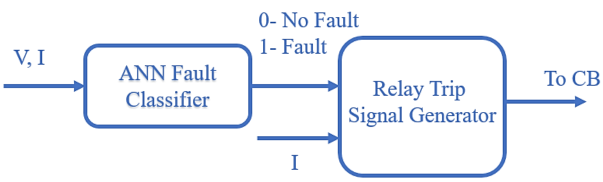

Figure 7. Integrated system approach to reduce circuit breaker nuisance tripping

Table 5. Relay setting of CB's with and without RFSCL

Relay	Without RSFCL		With RSFCL	
	TD	PS	TD	PS
RCB2	0.3123	1.76	0.3010	1.87
RCB4	2.6632	6.19	2.5671	5.73
RCB1	5.0316	5.65	4.8508	5.27

5. CONCLUSION

In conclusion, this study has made significant strides in advancing fault diagnosis and protection in DG-connected electrical systems, employing a combination of resistive superconducting fault current limiters (RSFCL) and artificial neural network (ANN)-based fault identification methods. The various insights of the study are as follows: i) strategic placement of RSFCL within the distribution network can be done by carefully considering factors such as fault current magnitude, voltage quality, and resistance value, to reduce the maximum resistance value while maintaining fault current limitation. Position P1-P2 with a maximum resistance of 20 Ω is selected based on this tradeoff. P1-P2 shows a CRR of 57.79% for Symmetrical fault F1 and 82.16% for symmetrical fault F2. ii) The ANN-based fault diagnosis technique utilizing symmetrical components of current and voltage as electrical features has shown remarkable validation accuracy with a rate of 99.7%. This high level of precision is partly attributed to the careful analysis of feature variables, particularly addressing multicollinearity. By identifying and subsequently eliminating highly correlated variables, such as 'v2n' due to its substantial correlation of 0.81 with another feature, the model's robustness and effectiveness were significantly enhanced. iii) The decision to activate a circuit breaker is confirmed by the ANN, which means it only trips when the ANN detects a real fault. This is more accurate than older methods that trip based on simple preset limits. iv) However, the current study is limited to incorporating the thermal and electrical properties of RFSCL and the transient stability of the system with RFSCL placement. The ANN is trained for various fault types with and without RSFCL and DG. In the future, the proposed framework can be extended to consider varying DG penetration levels, renewable intermittency, and real-time dynamics, along with hybrid AI models such as CNN–LSTM for improved temporal fault detection. Furthermore, adaptive and self-learning protection schemes that evolve with changing network topology and smart grid architectures remain a promising direction for advancing the reliability of DG-connected systems.

FUNDING INFORMATION

No funding involved.

AUTHOR CONTRIBUTIONS STATEMENT

This journal uses the Contributor Roles Taxonomy (CRediT) to recognize individual author contributions, reduce authorship disputes, and facilitate collaboration.

Name of Author	C	M	So	Va	Fo	I	R	D	O	E	Vi	Su	P	Fu
Lekshmi R. Chandran	✓	✓	✓	✓	✓	✓		✓	✓	✓			✓	
Ilango Karuppasamy		✓				✓		✓	✓	✓	✓	✓		
Manjula G. Nair		✓	✓	✓			✓			✓	✓		✓	✓

C : **C**onceptualization
M : **M**ethodology
So : **So**ftware
Va : **Va**lidation
Fo : **Fo**rmal analysis
I : **I**nvestigation
R : **R**esources
D : **D**ata Curation
O : Writing - **O**riginal Draft
E : Writing - Review & **E**diting
Vi : **Vi**sualization
Su : **Su**pervision
P : **P**roject administration
Fu : **Fu**nding acquisition

CONFLICT OF INTEREST STATEMENT

The authors declare that they have no known competing financial interests or personal relationships that could have influenced the work reported in this paper. The authors declare no conflict of interest.

DATA AVAILABILITY

The data that support the findings of this study are available from the corresponding author, [LRC], upon reasonable request.

REFERENCES

[1] C. D. Iweh, S. Gyamfi, E. Tanyi, and E. Effah-Donyina, "Distributed generation and renewable energy integration into the grid: prerequisites, push factors, practical options, issues and merits," *Energies*, vol. 14, no. 17, 2021, doi: 10.3390/en14175375.

[2] M. Singh, "Protection coordination in distribution systems with and without distributed energy resources- a review," *Protection and Control of Modern Power Systems*, vol. 2, no. 1, 2017, doi: 10.1186/s41601-017-0061-1.

[3] R. F. Arritt and R. C. Dugan, "Review of the impacts of distributed generation on distribution protection," in *Papers Presented at the Annual Conference - Rural Electric Power Conference*, 2015, pp. 69–74, doi: 10.1109/REPC.2015.12.
[4] K. Aseem and S. S. Kumar, "High temperature superconducting material based energy storage for solar-wind hybrid generating systems for fluctuating power management," *Materials Today: Proceedings*, vol. 42, pp. 1122–1129, 2021, doi: 10.1016/j.matpr.2020.12.493.
[5] "Fault current limiters report on the activities of CIGRE WG A3.10 by CIGRE Working Group 13.10 (*)," [Online]. Available: https://api.semanticscholar.org/CorpusID:276601939.
[6] American Superconductor Corporation (AMSC), "Application guide for ac high-temperature superconducting (HTS) cables," 2020. [Online]. Available: https://www.amsc.com/wp-content/uploads/Application-Guide-for-Superconductor-Cables-19FEB2020.pdf.
[7] V. V. Rao and S. Kar, "Superconducting fault current limiters - a review," *Indian Journal of Cryogenics*, vol. 36, no. 1–4, pp. 14–25, 2011.
[8] M. S. Alam, M. A. Y. Abido, and I. M. El-Amin, "Fault current limiters in power systems: a comprehensive review," *Energies*, vol. 11, no. 5, 2018, doi: 10.3390/en11051025.
[9] G. García, D. M. Larruskain, and A. Etxegarai, "Modelling of resistive type superconducting fault current limiter for hvdc grids," *Energies*, vol. 15, no. 13, 2022, doi: 10.3390/en15134605.
[10] S. Eckroad, "Superconducting fault current limiters," *Electric Power Research Institute*, p. 1017793, 2009.
[11] S. Yadav, G. K. Choudhary, and R. Kumar Mandal, "Review on fault current limiters," *International Journal of Engineering Research & Technology (IJERT)*, vol. 3, no. 4, pp. 1595–1603, 2014, doi: 10.17577/IJERTV3IS041493.
[12] N. Naufal, P. K. Preetha, and V. Sruthy, "Reliability enhancement of an interconnected power system using fault current limiter," in *2017 Innovations in Power and Advanced Computing Technologies (i-PACT)*, Vellore, India, 2017, pp. 1–6, doi: 10.1109/IPACT.2017.8244972.
[13] N. Naufal, P. K. Preetha, and V. Sruthy, "Dynamic analysis of converter based fault current limiter of an AC/DC microgrid," in *2017 International Conference on Technological Advancements in Power and Energy (TAP Energy)*, IEEE, Dec. 2017, pp. 1–5, doi: 10.1109/TAPENERGY.2017.8397226.
[14] A. Abramovitz, K. M. Smedley, F. De La Rosa, and F. Moriconi, "Prototyping and testing of a 15 kV/1.2 kA saturable core hts fault current limiter," *IEEE Transactions on Power Delivery*, vol. 28, no. 3, pp. 1271–1279, 2013, doi: 10.1109/TPWRD.2013.2256801.
[15] S. Eckroad, "Superconducting power equipment: technology watch," *Electric Power Research Institute*, 2012.
[16] D. Chen *et al.*, "A novel solution for fault current suppression in transmission systems based on fault current splitters," *Electric Power Systems Research*, vol. 194, 2021, doi: 10.1016/j.epsr.2021.107050.
[17] P. Wang, W. Wei, Z. Mao, X. Hao, W. Wang, and D. Xu, "Proposal and verification of a novel dc solid-state fault current limiter," in *ICEMS 2021 - 2021 24th International Conference on Electrical Machines and Systems*, 2021, pp. 2156–2160, doi: 10.23919/ICEMS52562.2021.9634383.
[18] H. Y. Lee, M. Asif, K. H. Park, and B. W. Lee, "Feasible application study of several types of superconducting fault current limiters in HVDC grids," *IEEE Transactions on Applied Superconductivity*, vol. 28, no. 4, 2018, doi: 10.1109/TASC.2018.2799745.
[19] R. Tan, Y. Wang, and S. Zhang, "Coordination scheme of SFCL and SMES in the DC microgrid for fault current limiting and voltage stability," in *2020 IEEE International Conference on Applied Superconductivity and Electromagnetic Devices, ASEMD 2020*, 2020, doi: 10.1109/ASEMD49065.2020.9276114.
[20] V. B. Vaishnavi, A. R. S. Suji, D. T. Privenishree, N. Nabi, and G. J. Sowmya, "Superconducting fault current limiter & its application," *International Journal of Scientific & Engineering Research*, vol. 7, no. 5, pp. 126–134, 2016.
[21] A. Etxegarai, I. Zamora, G. Buigues, V. Valverde, E. Torres, and P. Eguia, "Models for fault current limiters based on superconductor materials," *Renewable Energy and Power Quality Journal*, vol. 1, no. 14, pp. 284–289, 2016, doi: 10.24084/repqj14.293.
[22] J. C. H. Llambes, D. W. Hazelton, and C. S. Weber, "Recovery under load performance of 2nd generation hts superconducting fault current limiter for electric power transmission lines," *IEEE Transactions on Applied Superconductivity*, vol. 19, no. 3, pp. 1968–1971, 2009, doi: 10.1109/TASC.2009.2018519.
[23] S. Saha, J. Pradhan, R. Bhar, and A. D. Gupta, "Development of HTS current lead for cryo-cooler based superconducting magnet," *Indian Journal of Cryogenics*, vol. 50, no. 1, pp. 40–44, 2025, doi: 10.5958/2349-2120.2025.00008.2.
[24] M. A. Mohamed and A. M. Emad, "Enhancement of multi-machine power system transient stability using superconducting fault current limiters with YBCO and Bi-2212," *International Journal on Power Engineering and Energy (IJPEE)*, vol. 5, pp. 418–423, 2014.
[25] F. Tariverdi and A. Doroudi, "Selection of resistive and inductive superconductor fault current limiters location considering system transient stability," *Journal of Electric Power and Energy Conversion Systems*, vol. 1, no. 72–78, 2016.
[26] L. R. Chandran, K. Ilango, M. G. Nair, A. A. Kumar, A. A. Kumar, and M. Adithya Raj, "Multilabel external fault classification of induction motor using machine learning models," in *Proceedings of the 2022 3rd International Conference on Intelligent Computing, Instrumentation and Control Technologies: Computational Intelligence for Smart Systems, ICICICT 2022*, 2022, pp. 559–564, doi: 10.1109/ICICICT54557.2022.9917882.
[27] A. Srivastava and S. K. Parida, "A robust fault detection and location prediction module using support vector machine and Gaussian process regression for ac microgrid," *IEEE Transactions on Industry Applications*, vol. 58, no. 1, pp. 930–939, 2022, doi: 10.1109/TIA.2021.3129982.
[28] V. Negri, A. Mingotti, R. Tinarelli, and L. Peretto, "Comparison of algorithms for the AI-based fault diagnostic of cable joints in MV networks," *Energies*, vol. 16, no. 1, 2023, doi: 10.3390/en16010470.
[29] O. Mey and D. Neufeld, "Explainable AI algorithms for vibration data-based fault detection: use case-adapted methods and critical evaluation," *Sensors*, vol. 22, no. 23, 2022, doi: 10.3390/s22239037.
[30] S. M. Blair, C. D. Booth, and G. M. Burt, "Current-time characteristics of resistive superconducting fault current limiters," *IEEE Transactions on Applied Superconductivity*, vol. 22, no. 2, 2012, doi: 10.1109/TASC.2012.2187291.
[31] M. T. Chen and C. H. Nguyen, "Voltage quality performance improvement of a distribution feeder with superconducting fault current limiter," *International Journal on Electrical Engineering and Informatics*, vol. 7, no. 1, pp. 102–117, 2015, doi: 10.15676/ijeei.2015.7.1.8.
[32] M. Khatibi and M. Bigdeli, "Transient stability improvement of power systems by optimal sizing and allocation of resistive superconducting fault current limiters using particle swarm optimization," *Advanced Energy: An International Journal (AEIJ)*, vol. 1, no. 3, 2014.
[33] L. Chen *et al.*, "Study of resistive-type superconducting fault current limiters for a hybrid high voltage direct current system," *Materials*, vol. 12, no. 1, 2018, doi: 10.3390/ma12010026.
[34] J. Bock, A. Hobl, J. Schramm, S. Kramer, and C. Janke, "Resistive superconducting fault current limiters are becoming a mature technology," *IEEE Transactions on Applied Superconductivity*, vol. 25, no. 3, 2015, doi: 10.1109/TASC.2014.2364916.

[35] H. S. Ruiz, X. Zhang, and T. A. Coombs, “Resistive-type superconducting fault current limiters: concepts, materials, and numerical modeling,” *IEEE Transactions on Applied Superconductivity*, vol. 25, no. 3, 2015, doi: 10.1109/TASC.2014.2387115.
[36] L. Ye and K. P. Juengst, “Modeling and simulation of high temperature resistive superconducting fault current limiters,” *IEEE Transactions on Applied Superconductivity*, vol. 14, no. 2, pp. 839–842, 2004, doi: 10.1109/TASC.2004.830293.
[37] J. Cui, C. Jia, L. Qu, and W. Qiao, “A tunable-inductor-based fault current limiter,” *IEEE Transactions on Industry Applications*, vol. 61, no. 3, pp. 4992–5002, 2025, doi: 10.1109/TIA.2025.3540730.
[38] Z. Esmaeili and H. Heydari, “A review of the effect of common fault current limiters (FCLs) on power systems reliability,” *The Journal of Engineering*, vol. 2025, no. 1, 2025, doi: 10.1049/tje2.70057.
[39] M. H. Sadeghi, Y. Damchi, and H. Shirani, “Improvement of operation of power transformer protection system during sympathetic inrush current phenomena using fault current limiter,” *IET Generation, Transmission and Distribution*, vol. 12, no. 22, pp. 5968–5974, 2018, doi: 10.1049/iet-gtd.2018.5697.
[40] S. H. Lim, J. S. Kim, and J. C. Kim, “Analysis on protection coordination of hybrid SFCL with protective devices in a power distribution system,” *IEEE Transactions on Applied Superconductivity*, vol. 21, no. 3 PART 2, pp. 2170–2173, 2011, doi: 10.1109/tasc.2010.2093593.
[41] F. Zheng, C. Deng, L. Chen, S. Li, Y. Liu, and Y. Liao, “Transient performance improvement of microgrid by a resistive superconducting fault current limiter,” *IEEE Transactions on Applied Superconductivity*, vol. 25, no. 3, 2015, doi: 10.1109/TASC.2015.2391120.
[42] O. B. Hyun, “Brief review of the field test and application of a superconducting fault current limiter,” *Progress in Superconductivity and Cryogenics (PSAC)*, vol. 19, no. 4, pp. 1–11, 2017, doi: 10.9714/psac.2017.19.4.001.
[43] D. Klaus *et al.*, “Superconducting fault current limiters - UK network trials live and limiting,” in *IET Conference Publications*, 2013, doi: 10.1049/cp.2013.0650.
[44] R. Resmi, V. Vanitha, E. Aravind, B. R. Sundaram, C. A. Raj, and S. Harithaa, “Detection, classification and zone location of fault in transmission line using artificial neural network,” in *Proceedings of 2019 3rd IEEE International Conference on Electrical, Computer and Communication Technologies, ICECCT 2019*, 2019, doi: 10.1109/ICECCT.2019.8868990.
[45] N. G. Krishna, J. Raj, and L. R. Chandran, “Transmission line monitoring and protection with ANN aided fault detection, classification and location,” in *Proceedings - 2nd International Conference on Smart Electronics and Communication, ICOSEC 2021*, 2021, pp. 883–889, doi: 10.1109/ICOSEC51865.2021.9591911.
[46] A. S. Neethu and T. S. Angel, “Smart fault location and fault classification in transmission line,” in *2017 IEEE International Conference on Smart Technologies and Management for Computing, Communication, Controls, Energy and Materials, ICSTM 2017 - Proceedings*, 2017, pp. 339–343, doi: 10.1109/ICSTM.2017.8089181.
[47] R. S. Jawad and H. Abid, “HVDC fault detection and classification with artificial neural network based on ACO-DWT method,” *Energies*, vol. 16, no. 3, 2023, doi: 10.3390/en16031064.
[48] T. Biswal and S. K. Parida, “A novel high impedance fault detection in the micro-grid system by the summation of accumulated difference of residual voltage method and fault event classification using discrete wavelet transforms and a decision tree approach,” *Electric Power Systems Research*, vol. 209, 2022, doi: 10.1016/j.epsr.2022.108042.
[49] D. S. Kumar, B. M. Radhakrishnan, D. Srinivasan, and T. Reindl, “An adaptive fuzzy based relay for protection of distribution networks,” *IEEE International Conference on Fuzzy Systems*, 2015, doi: 10.1109/FUZZ-IEEE.2015.7338112.
[50] Y. D. Mamuya, Y. Der Lee, J. W. Shen, M. Shafiullah, and C. C. Kuo, “Application of machine learning for fault classification and location in a radial distribution grid,” *Applied Sciences (Switzerland)*, vol. 10, no. 14, 2020, doi: 10.3390/app10144965.
[51] B. Bhalja and R. P. Maheshwari, “Wavelet-based fault classification scheme for a transmission line using a support vector machine,” *Electric Power Components and Systems*, vol. 36, no. 10, pp. 1017–1030, Sep. 2008, doi: 10.1080/15325000802046496.
[52] S. V. Khond, “Effect of data normalization on accuracy and error of fault classification for an electrical distribution system,” *Smart Science*, vol. 8, no. 3, pp. 117–124, 2020, doi: 10.1080/23080477.2020.1799135.
[53] N. Mazibuko, K. T. Akindeji, and K. Moloi, “Performance comparison of machine learning (ML) based fault detection scheme for a compensated transmission line,” *2024 IEEE PES/IAS PowerAfrica, PowerAfrica 2024*, 2024, doi: 10.1109/PowerAfrica61624.2024.10759459.
[54] R. M. Souza, E. G. S. Nascimento, U. A. Miranda, W. J. D. Silva, and H. A. Lepikson, “Deep learning for diagnosis and classification of faults in industrial rotating machinery,” *Computers and Industrial Engineering*, vol. 153, 2021, doi: 10.1016/j.cie.2020.107060.
[55] V. N. Ogar, S. Hussain, and K. A. A. Gamage, “The use of artificial neural network for low latency of fault detection and localisation in transmission line,” *Heliyon*, vol. 9, no. 2, 2023, doi: 10.1016/j.heliyon.2023.e13376.
[56] D. Gutierrez-Rojas, P. H. J. Nardelli, G. Mendes, and P. Popovski, “Review of the state of the art on adaptive protection for microgrids based on communications,” *IEEE Transactions on Industrial Informatics*, vol. 17, no. 3, pp. 1539–1552, 2021, doi: 10.1109/TII.2020.3006845.
[57] A. M. Agwa and A. A. El-Fergany, “Protective relaying coordination in power systems comprising renewable sources: challenges and future insights,” *Sustainability (Switzerland)*, vol. 15, no. 9, 2023, doi: 10.3390/su15097279.
[58] L. R. Chandran, V. S. Anju Parvathy, K. Ilango, and M. G. Nair, “Adaptive over current relay protection in a PV penetrated radial distribution system with fuzzy GA optimisation,” in *INDICON 2022 - 2022 IEEE 19th India Council International Conference*, 2022, doi: 10.1109/INDICON56171.2022.10040021.
[59] F. Alasali *et al.*, “Advanced coordination method for overcurrent protection relays using new hybrid and dynamic tripping characteristics for microgrid,” *IEEE Access*, vol. 10, pp. 127377–127396, 2022, doi: 10.1109/ACCESS.2022.3226688.
[60] A. Reda, A. F. Abdelgawad, M. I. Elsayed, and F. B. Al-Dousar, “Multi-characteristic overcurrent relay of feeder protection for minimum tripping times and self-protection,” *Electrical Engineering*, vol. 105, no. 2, pp. 605–617, 2023, doi: 10.1007/s00202-022-01683-5.
[61] M. Usama *et al.*, “A multi-objective optimization of FCL and DOCR settings to mitigate distributed generations impacts on distribution networks,” *International Journal of Electrical Power and Energy Systems*, vol. 147, 2023, doi: 10.1016/j.ijepes.2022.108827.
[62] O. Merabet, A. Kheldoun, M. Bouchahdane, A. Eltom, and A. Kheldoun, “An adaptive protection coordination for microgrids utilizing an improved optimization technique for user-defined DOCRs characteristics with different groups of settings considering N-1 contingency,” *Expert Systems with Applications*, vol. 248, 2024, doi: 10.1016/j.eswa.2024.123449.
[63] A. S. Mohamed, D. Kundur, and M. Khalaf, “A probabilistic approach to adaptive protection in the smart grid,” *ACM Transactions on Cyber-Physical Systems*, vol. 9, no. 1, 2025, doi: 10.1145/3656347.

APPENDIX

Table 3. Performance analysis of the test system with various RSFCL values at various fault positions for symmetrical fault

Fault positions		Symmetrical fault – F1						Symmetrical fault – F2					
RFSCL position	SFCL resistance (Ω)	Grid voltage (V)	Grid current (A)	DG current (A)	Fault current (A)	CRR (%)	VSP (%)	Grid voltage (V)	Grid current (A)	DG current (A)	Fault current (A)	CRR (%)	VSP (%)
No RFSCL	0	90	4510	1551	6062			90	4539	1561	6099		
P1	5	6193	3504	1551	4889	19.35	43.70	6140	4510	1561	4906	19.77	44.18
	10	8630	2477	1551	3685	39.21	21.55	8631	2477	1561	3701	39.48	21.54
	20	10110	1455	1551	2573	57.56	8.09	10110	1455	1561	2575	57.89	8.09
	30	10530	1011	1551	2145	64.62	4.27	10530	1011	1561	2145	64.92	4.27
	40	10710	772	1551	1944	67.93	2.64	10710	772	1561	1944	68.21	2.64
P2	5	90	4510	1551	6062	0.00	99.18	7264	3081	1079	4158	32.00	33.96
	10	90	4510	1551	6062	0.00	99.18	9374	1989	708	2695	55.93	14.78
	20	90	4510	1551	6062	0.00	99.18	10410	1098	404	1500	75.47	5.36
	30	90	4510	1551	6062	0.00	99.18	10690	745	284	1027	83.21	2.82
	40	90	4510	1551	6062	0.00	99.18	10810	561	221	779	87.26	1.73
P3	5	90	4510	1522	6018	0.73	99.18	91	4510	1522	6018	1.59	99.17
	10	90	4510	1470	5918	2.38	99.18	91	4510	1470	5943	2.81	99.17
	20	90	4510	1333	5711	5.79	99.18	91	4510	1333	5738	6.17	99.17
	30	90	4510	1184	5495	9.35	99.18	91	4510	1184	5523	9.68	99.17
	40	90	4509	1047	5335	11.99	99.18	91	4510	1047	5335	12.76	99.17
P1-P2	5	6139	3504	1551	4901	19.15	44.19	9492	2275	1021	3196	47.74	13.71
	10	8603	2477	1551	3685	39.21	21.79	10890	1267	806	1906	68.83	1.00
	20	10110	1455	1551	2559	57.79	8.09	11210	607	661	1091	82.16	-1.91
	30	10530	1011	1551	2145	64.62	4.27	11390	367	564	811	86.74	-3.55
	40	10710	772	1551	1944	67.93	2.64	11330	360	419	665	89.13	-3.00
P2-P3	5	90	4150	1522	6018	0.73	99.18	7139	3053	1044	4087	33.16	35.10
	10	90	4510	1470	5943	1.96	99.18	9131	1981	664	2624	57.09	16.99
	20	90	4150	1333	5739	5.33	99.18	10410	1098	404	1500	75.47	5.36
	30	90	4510	1184	5495	9.35	99.18	10690	745	284	1027	83.21	2.82
	40	90	4510	1047	5335	11.99	99.18	10810	561	221	779	87.26	1.73
P1-P3	5	6139	3504	1521	4903	19.12	44.19	6141	3504	1521	4930	19.38	44.17
	10	8630	2477	1469	3773	37.76	21.55	8631	2477	1469	3773	38.30	21.54
	20	10110	1455	1332	2633	56.57	8.09	10110	1455	1332	2633	56.94	8.09
	30	10530	1011	1184	2094	65.46	4.27	10530	1011	1184	2094	65.76	4.27
	40	10710	771	1047	1754	71.07	2.64	10710	771	1047	1754	71.32	2.64

Table 3. Performance analysis of the test system with various RSFCL values at various fault positions for symmetrical fault (continued)

Fault positions		Symmetrical fault – F1						Symmetrical fault – F2					
RFSCL position	SFCL resistance (Ω)	Grid voltage (V)	Grid current (A)	DG current (A)	Fault current (A)	CRR (%)	VSP (%)	Grid voltage (V)	Grid current (A)	DG current (A)	Fault current (A)	CRR (%)	VSP (%)
P1-P2-P3	5	6139	3504	1521	4930	18.67	44.19	9414	2247	985	3173	48.11	14.42
	10	8630	2477	1470	3773	37.76	21.55	10730	1228	736	1882	69.22	2.45
	20	10110	1455	1322	2633	56.57	8.09	11100	573	530	1047	82.88	-0.91
	30	10530	1011	1184	2095	65.44	4.27	11190	357	435	745	87.82	-1.73
	40	10710	771	1047	1754	71.07	2.64	11240	363	398	674	88.98	-2.18

BIOGRAPHIES OF AUTHORS

Lekshmi R. Chandran received B.Tech. in Electrical and Electronics Engineering from Amrita University in 2011 and M.Tech. in Power Electronics from Amrita University in 2013. She currently serves as an assistant professor in the Department of Electrical and Electronics Engineering at Amrita School of Engineering, Amritapuri, India. She published more than 25 academic articles. Her research interests include artificial intelligence applications in smart grid, image processing applications in smart grid, smart grid monitoring and protection, compressive sensing applications, power quality monitoring, and power electronics applications in smart grid. She serves as a reviewer of reviewer of Journal of Industrial Information Integration, Engineering Applications of Artificial Intelligence, Neural Computing and Applications, and other peer-reviewed journals. She can be contacted at email: lekshmichandran@am.amrita.edu.

Ilango Karuppasamy completed his B.E. degree in Electrical and Electronics Engineering from Madurai Kamaraj University in 2002, Master of Engineering in Power Systems from PSG College of Technology, Coimbatore, Anna University in 2004. He pursued Ph.D. in the area of electrical engineering and the work titled on “Grid integration of renewable energy sources with power quality improvement” from Amrita Vishwa Vidyapeetham in 2016. He is currently serving as an associate professor in the Department of Electrical and Electronics Engineering, School of Engineering, Amrita Vishwa Vidyapeetham, Coimbatore. He has 19 years of rich teaching experience and 15 years of research experience. He has been associated with Amrita Vishwa Vidyapeetham since 2008. He has published articles in more than 70+ international journal/conference publications. He has been serving as a reviewer of Elsevier, IEEE Access, IET Power Electronics, Journal of Systems and Control Engineering, and other peer-reviewed journals. Dr. Ilango has been the recipient of the Amrita-TIDE Innovative Project Award and Amrita TBI Best Idea Award and also got a grant for the implementation of project work. He is an active senior member of IEEE/Power and Energy Society, IEEE SIGHT and a life member of ISTE. His current research interest includes integration of renewable energy sources and power quality, energy management of microgrids, and energy conservation and management. He can be contacted at email: k_ilango@cb.amrita.edu.

Manjula G. Nair received Ph.D. in Power Electronics and Drives from the Indian Institute of Technology Delhi, M.Tech. in electric power systems, and B.Tech. in Electrical and Electronics Engineering from Calicut University. She currently serves as professor and chairperson in the Department of Electrical and Electronics Engineering, School of Engineering, Amrita Vishwa Vidyapeetham, Coimbatore, of the Department of EEE at Amritapuri Campus. She has more than 28 years of experience in teaching and research with more than 100 research publications. Her research includes research interests are in electric vehicles-charging stations and grid integration, smart zero net energy buildings and smart devices, smart grids, renewable energy systems, FACTS and power quality improvement, hybrid energy storage systems, AI/IoT/multi agent systems applications in smart grids and autonomous vehicles. She serves as a reviewer of research publications of IEEE Transactions in Industrial Electronics, Power Delivery, Smart Grids, and many Elsevier journals. She also serves as an AICTE reviewer for STTPs and other funded project proposals. She worked on the funded project on digital hybrid filtering for power quality improvement, funded by Department of Science and Technology (DST), Ministry of Human Resource Development (MHRD), Government of India. She can be contacted at email: manjulagnair@am.amrita.edu.